Cao et al. *Zool. Res.* 2023, 44(2): 259−268
https://doi.org/10.24272/j.issn.2095-8137.2022.330

ZR | Zoological Research

Article Open Access

Transfer of the *zp3a* gene results in changes in egg adhesiveness and buoyancy in transgenic zebrafish

Yu-Qing Cao[1,3], Yong-Xin Wang[1,3], Yan Zhao[3,4], Jia Zhang[3,4], Xian He[1,3], Ping Xie[4], Jun Chen[4,*], Yu-Hua Sun[1,2,3,*]

[1] *Institute of Hydrobiology*, *Chinese Academy of Sciences*, *Wuhan*, *Hubei* 430072, *China*
[2] *Innovation Academy for Seed Design*, *Chinese Academy of Sciences*, *Beijing* 100049, *China*
[3] *University of Chinese Academy of Sciences*, *Beijing* 100049, *China*
[4] *Donghu Experimental Station of Lake Ecosystems*, *State Key Laboratory of Freshwater Ecology and Biotechnology*, *Institute of Hydrobiology*, *Chinese Academy of Sciences*, *Wuhan*, *Hubei* 430072, *China*

ABSTRACT

Reproductive strategies and spawning habits play key roles in the evolution of endemic East Asian cyprinids. However, the molecular mechanisms underlying the regulation of spawning habits are not well understood. We recently identified zona pellucida (Zp) as the top differentially expressed protein between East Asian cyprinids that produce adhesive and semi-buoyant eggs, suggesting that Zp protein may play important roles in the regulation of egg type. In this work, we generated transgenic zebrafish in which oocyte-specific expression of *zp* genes from rare minnow (*Gobiocypris rarus*), an East Asian cyprinid laying adhesive eggs, was driven by a zebrafish *zp3.2* gene promoter. We found that the transgenic eggs obtained partial adhesiveness and exhibited alteration in hydration and buoyancy. Abnormal metabolism of vitellogenin (VTG) may contribute to enhanced hydration and/or buoyancy. Our work shows that expression of the exogenous *zp3a* gene from an adhesive-egg producing fish is sufficient to induce changes in both egg adhesiveness and buoyancy in zebrafish, emphasizing the important role of *zp* genes in the regulation of spawning habits. Our results thus provide new insights into how endemic East Asian cyprinids may have adapted to the Yangtze river-lake system via changes in spawning habits.

Keywords: Zona pellucida protein; Adhesive; Buoyancy; Hydration; Egg envelope

INTRODUCTION

Cyprinidae is one of the largest fish families in the world, with the highest species diversity found in East Asia (Kong et al., 2007). The development of the cross-linked river-lake system, shaped by uplift of the Qinghai-Xizang (Tibet) Plateau and East Asian monsoon, greatly increased the ecological and phenotypic diversity of the endemic East Asian cyprinids within a relatively short time, enabling them to exploit areal lakes and river drainages, resulting in rapid species diversification (Feng et al., 2022; Sun & Wang, 2005; Wang & Wu, 2015).

Mitochondrial DNA-based phylogenetic analysis revealed that the endemic East Asian cyprinid clade evolved diverse spawning habits and reproductive strategies (producing adhesive, demersal, and semi-buoyant eggs) (Chen et al., 2022; Tao et al., 2010). Demersal eggs appeared approximately 22 million years ago (Ma), followed by semi-buoyant eggs (18 Ma) and adhesive eggs (14 Ma), coincident with the formation of the Yangtze river-lake system during the mid-Miocene and the burst of diversification of East Asian cyprinids (Chen et al., 2022; Zheng, 2015). Studies support the notion that traits related to spawning habits play a major role in shaping biodiversity during adaptive radiation (Marques et al., 2019; McGee et al., 2020). However, the molecular mechanisms underlying the regulation of spawning habits remain unclear.

The egg envelope (EE) in vertebrates is transparent and called the zona pellucida (ZP) (Bonsignorio et al., 1996). The acellular egg envelope surrounding teleost oocytes serves multiple functions, including nutrient and water uptake, functional buoyancy, embryo protection, species-specific sperm binding, sperm guidance to the micropyle, and a barrier to contaminants and microorganisms (Mansour et al., 2009). Microstructural analysis using transmission electron microscopy has shown that semi-buoyant eggs, which undergo hydration to adapt to fast-flowing rivers, consist of three-layer structures in the EE, while adhesive eggs, which adhere to water plants in lakes, often consist of four layers (Bonsignorio et al., 1996; Chen et al., 2022; Esmaeili &Johal, 2005; Rizzo et al., 2002; Sano et al., 2017). For adhesive eggs, the outer surface of the EE develops an adhesive layer

Received: 30 November 2022; Accepted: 13 January 2023; Online: 13 January 2023
Foundation items: This work was supported by the Strategic Priority Research Program of the Chinese Academy of Sciences (XDB31000000)
*Corresponding authors, E-mail: sunyh@ihb.ac.cn; chenjun@ihb.ac.cn

after fertilization or activation (Murray et al., 2013). Although the biochemistry of the adhesive substances remains unclear, glycoprotein and glycosaminoglycan (GAG) are implicated in their formation (Mansour et al., 2009; Niksirat et al., 2017, 2020).

The ZP consists of 2–4 major Zp proteins that are relatively conserved among vertebrate species. Recent studies suggest that ZPs may have additional functions other than as a component within the EE. For instance, ZP3 is concentrated in the nucleus and plays an important role in germinal vesicle breakdown required for mouse oocyte meiosis and maturation (Gao et al., 2017). Furthermore, ZPs in the EE can enhance freezing resistance of Antarctic notothenioid eggs (Cao et al., 2016).

In the current study, we performed multi-omics analysis of developing oocytes in the rare minnow (*Gobiocypris rarus*), a cyprinid species that lays adhesive eggs, and identified *zp* genes as the top differentially expressed genes (DEGs) closely associated with spawning habits. We hypothesized that Zp proteins play important roles in the regulation of egg adhesiveness and reasoned that expressing rare minnow Zp in zebrafish eggs may result in changes in egg type. Using transgenic zebrafish, we found that expression of the rare minnow Zp3a protein not only altered egg adhesiveness, but also buoyancy.

MATERIALS AND METHODS

Zebrafish maintenance

Zebrafish (*Danio rerio*) were obtained from the China Zebrafish Resource Center (Wuhan, China). Fish were maintained at 28.5 °C in 10 L tanks on a 12 h light/12 h dark cycle and were fed with brine shrimp twice a day. Fertilized eggs were obtained by natural breeding. All procedures were performed with the approval of the Institute of Hydrobiology, Chinese Academy of Sciences (CAS), Wuhan, China.

Generation of transgenic zebrafish lines

We aimed to generate transgenic zebrafish lines in which EE-enriched Zp proteins from rare minnow were stably expressed in oocytes or eggs. To achieve oocyte-specific expression of rare minnow *zp* genes, we used a previously reported zebrafish *zp3.2* promoter (Liu et al., 2006). The Tol2 transposon system developed by the Kawakami Laboratory was used to generate the transgenic zebrafish lines (Kawakami et al., 2004). Briefly, the pT2AL200R150G transposon vector was double-digested with XhoI and BamHI, and the ef1α promoter and β-globin intron were replaced with the zebrafish *zp3.2* promoter and rare minnow *zp* gene in frame with enhanced green fluorescent protein (eGFP) sequences. The transposon vector was injected together with transposase mRNA into one cell stage zebrafish eggs. The transgene was confirmed by polymerase chain reaction (PCR) or by examining eGFP signals in transgenic juveniles at 15–20 days post fertilization (dpf).

Rare minnow maintenance

Rare minnow (*Gobiocypris rarus*) were obtained from the Institute of Hydrobiology, CAS (Wuhan, China). Fish were maintained at 25±0.5 °C in 10 L tanks under a 12 h light/12 h dark cycle in the lab (Hu et al., 2022).

Genome sequencing and assembly of rare minnow

Rare minnow whole-genome DNA was extracted from muscle using a DNeasy Blood & Tissue kit (Qiagen, Germany). The quality of the extracted genomic DNA was examined using an Agilent 2100 Bioanalyzer (Agilent Technologies, USA). The libraries for DNA sequencing were constructed and sequenced on the Nanopore platform by the Novogene Company (China).

Genome assembly and evaluation were also performed by Novogene. To assess the integrity and accuracy of the assembled genome, several strategies including core gene complement, read mapping ratio, and expressed transcript mapping ratio were used. First, the eukaryotic and metazoan core gene complements were identified using BUSCO (v2.0). Second, all filtered short reads were mapped to the assembled genome using BWA software (v0.7.12) with default parameters to determine genome integrity and accuracy. Position depths were calculated using the “depth” command in SAMtools (v1.3.1). The rare minnow genome was bound into non-overlapping windows (window size of 10 kb), and any window with N content >0.1 was filtered. GC content and average sequencing depth in each window were then calculated and plotted. Third, all RNA sequencing (RNA-seq) reads from five different tissues/organs (gill, head kidney, kidney, liver, and spleen) were assembled using Bridger (r2014-12-01), with three repeats for each tissue/organ, and the assembled transcripts were then mapped to the genome using BLASTn (v2.3.0) with an E-value set to 10^{-5}. Blast results with an identity of more than 85% were selected, and the mapping ratio of all transcripts was calculated and plotted using R.

Generation of rare minnow mutants

We designed a gRNA targeting exon 1 of the *zp3a* gene of rare minnow (gRNA sequence 5’-GGCCCAGTGTTGGGAAG ATG-3’). Using CRISPR/Cas9 technology, we generated two mutant alleles, with one bearing a 2 bp deletion and one bearing a 5 bp deletion. The genotypes were determined by DNA sequencing.

Immunofluorescence (IF) assay

Fertilized eggs of transgenic and wild-type (WT) zebrafish were disrupted by forceps under a microscope. The EEs were fixed in 4% paraformaldehyde (PFA) in phosphate-buffered saline (PBS) at 4 °C overnight. After washing in PBS, the EEs were incubated in 1% normal goat serum in PBS for 1 h, followed by incubation with primary antibody (anti-FLAG, Sigma, F1804, USA) diluted 1:1 000 in 1% normal goat serum in PBS at 4 °C overnight. After washing in PBS, the samples were incubated for 50 min at room temperature with a fluorescein isothiocyanate (FITC)-conjugated secondary antibody. Finally, images were taken under a confocal microscope (Leica, Germany).

Hematoxylin and eosin (H&E) staining

For histological analysis, we dissected intact ovaries of 8-month-old rare minnow, and fixed them in 4% PFA/PBS overnight at 4 °C. After dehydration, samples were embedded in paraffin and cut into 4 μm thick slices. The slices were then stained with H&E (Servicebio Company, China).

Water content determination

Weighed eggs (wet mass, *Wm*, g, *n*=3 to 5, 1–3 g per replicate) were lyophilized in a vacuum freeze drier (ALPHA 1-4, Christ, Germany). After 48 h, dry mass (*Wd*, g) was

determined with a milli-balance (BSA124S, Sartorius, Germany) and the eggs were stored in a desiccator. Egg water content was calculated using the following equation:

$$\text{Water content}\ (\%) = 100(W_m - W_d)/W_m \qquad (1)$$

Transmission electron microscopy (TEM)

For TEM, fish eggs were prefixed in 2.5% glutaraldehyde solution, then fixed in 1% aqueous osmium tetroxide. The specimens were embedded in Epon-Araldite after dehydration. Ultrathin sections were cut with diamond knives on an EM UC7 ultramicrotome (Leica, Germany), then treated with contrast agents uranyl acetate and lead citrate. Images were taken on a Tecnai G2 20 TWIN microscope (FEI, USA).

Tandem mass tag (TMT)-based and label-free quantitative proteomic analysis

TMT-based quantitative proteomics and label-free quantitative proteomics were performed by Novogene (China). Samples in lysis buffer (8 mol/L urea, 1% Protease Inhibitor Cocktail) were placed on ice and sonicated three times using a high-intensity ultrasonic processor (Scientz Bio-tech, Ningbo, China). The remaining debris was removed by centrifugation at 12 000 ×*g* and 4 °C for 10 min. The supernatant was collected, and protein concentration was determined using a BCA kit (Beyotime, China) according to the manufacturer's instructions. Subsequently, 100 μg of protein from each sample was reduced with dithiothreitol, alkylated with iodoacetamide, digested with trypsin, and labeled with TMT reagents (Thermo, USA). The tryptic peptides were fractionated by high-pH reverse-phase high-performance liquid chromatography (HPLC) using an Agilent 300Extend-C18 column. The peptides were subjected to a nanospray ionization (NSI) source, followed by tandem mass spectrometry (MS/MS) using a Q Exactive™ Plus system (Thermo, USA) coupled online to an ultra-performance liquid chromatography (UPLC) system. Proteins in fish eggs and ovaries with a fold-change>1.2 and P<0.05, and proteins in the egg envelope with a fold-change>1.5 and P<0.05 were considered differentially expressed. For quality control purposes in egg proteomic analysis, mass errors and lengths of all peptides were analyzed. The distribution of mass errors was close to zero and mostly less than 10 ppm, indicating sufficient mass accuracy of the MS data. Furthermore, most peptides were between 8 and 20 amino acid residues in length, consistent with the properties of tryptic peptides, indicating that the results met the standard. For quality control purposes in EE proteomic analysis, mass errors were mostly less than 10 ppm, and most peptides were between 7 and 20 amino acid residues in length, indicating that the results met the standard.

Liquid chromatography-mass spectrometry (LC–MS) non-targeted metabolomics

Twelve groups of eggs (six control, and six transgenic) were collected and frozen for LC-MS non-targeted metabolomics analysis. Sample treatment and processing of raw data were performed in the LC-MS Metabolomics Center by the Anachro Company (China). Briefly, samples were incubated with internal standard in cold 80% methanol, then centrifuged at 16 000 ×*g* for 5 min at 4 °C to collect the supernatant. The supernatant were analyzed on a Dionex UHPLC Ultimate 3000 system (Thermo Fisher Scientific, USA) coupled to a Q Exactive™ mass spectrometer with a heated electrospray ionization (HESI) source and controlled by Xcalibur v2.3 (Thermo Fisher Scientific, USA). Chromatographic separation was performed on a Waters ACQUITY UPLC CSH C18 column (2.1 mm×100 mm, 1.8 μm) maintained at 35 °C. The mass spectrometry settings for positive/negative ionization modes were as follows: spray voltage, 3.8/−3.2 kV; sheath gas flow rate, 40 arbitrary units (arb); aux gas flow rate, 11/10 arb; aux gas heater temperature, 350 °C; capillary temperature, 300 °C; isolation width, 1 m/z.

Buoyancy testing experiment

The buoyancy experiments were performed as follows. Eggs from control and transgenic zebrafish were released at zero initial velocity at the center of a tank filled with egg water, approximately 1 cm below the water surface (so that eggs were not restrained by surface tension). As the eggs fell freely to the bottom, a camera was used to record the sinking process. The time from the surface to the bottom of the tank was counted. Velocity was calculated as distance (cm) divided by time (s). A total of 10 control and transgenic embryos were recorded at each time point.

Statistical analyses

Statistical analyses were performed using SPSS v25.0 (SPSS, USA). All values were presented as means±standard error of the mean (*SEM*). One-way analysis of variance (ANOVA) and Student *t*-tests were applied to determine the significance between control and transgenic groups. Significant values were set at P<0.05 (*), P<0.01 (**), and P<0.001 (***).

RESULTS

Zp proteins as candidates in regulation of egg adhesiveness

To identify candidate genes involved in the regulation of adhesiveness in rare minnow eggs, RNA-seq of oocytes at three developmental stages (early-, mid-, and late stages) was performed (Figure 1A). In total, 2 951 and 10 298 DEGs were identified between early- and mid-stage oocytes and between early- and late-stage oocytes, respectively (Figure 1B, C; Supplementary Figure S1A, B). KEGG (Kyoto Encyclopedia of Genes and Genomes) analysis of the 10 298 DEGs revealed enrichment in cell and focal adhesion, glycosaminoglycan synthesis, steroid hormone synthesis, c-type lectin receptor signaling, and endocytosis (Figure 1D). The top DEGs included the *zp*, *c-type lectin*, and *galactosaminyltransferase 1* genes. The *zp* genes were of particular interest to us, as they have been shown to be significantly up-regulated in the EEs of adhesive eggs compared to semi-buoyant eggs (Chen et al., 2022; Wang et al., 2022).

We next determined which Zps were abundantly expressed in the EE of rare minnow. To this end, label-free HPLC fractionation followed by LC-MS/MS analysis was conducted on the isolated EEs of ovulated eggs. Approximately 80 proteins were identified, including Zp, alpha-2-macroglobulin-like, and pregnancy zone proteins (Supplementary Figure S1). Four Zp proteins, homologous to zebrafish Zp3, Zp3a, Zp4-like (Zp4L), and Zp2L2, were highly represented (Figure 2A).

Using Cluster software, alignment of rare minnow Zps with zebrafish homologs revealed varying degrees of similarity. Zp3a is shown as a representative in Supplementary Figure S1C. Of note, rare minnow Zp3a contained two N-glycosylation sites, N*T and N*S, in the ZP core domain region, which were lacking in zebrafish Zp3a.

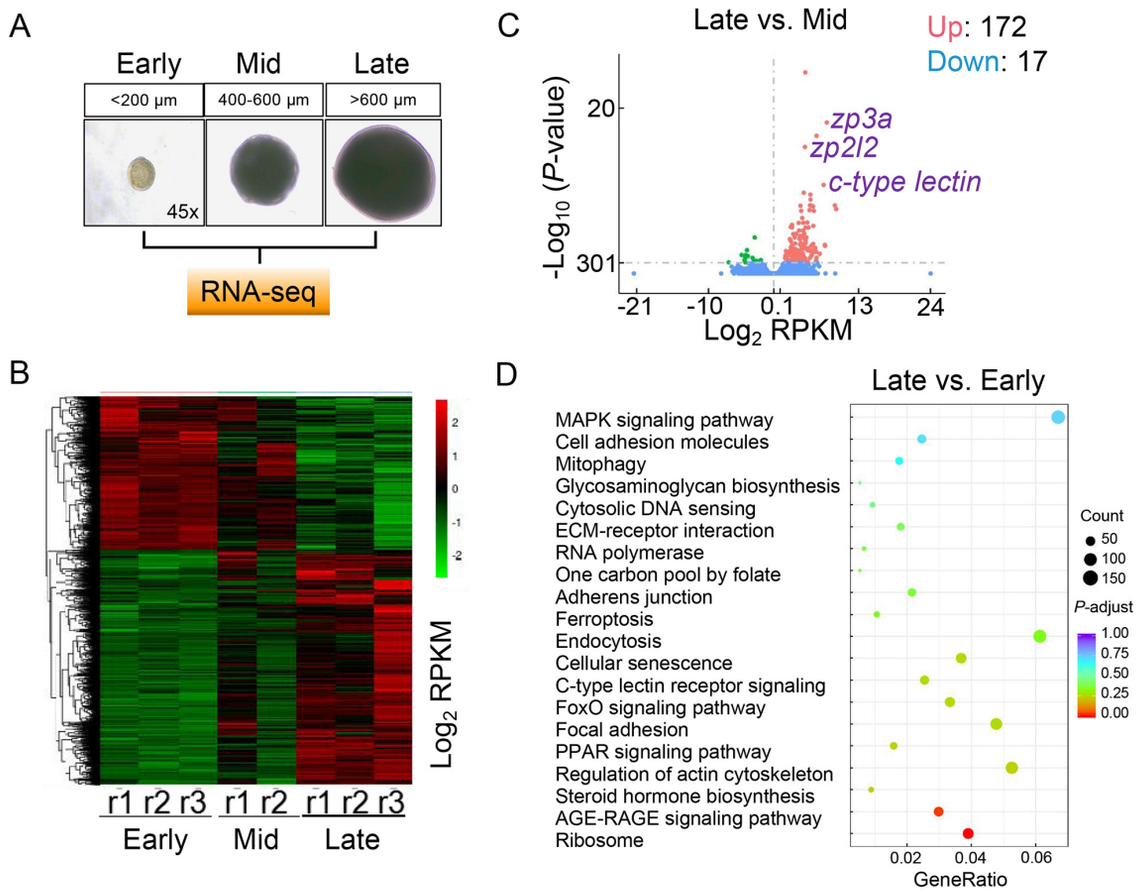

Figure 1 Identification of *zp* genes as candidates for regulation of egg adhesiveness

A: Cartoon showing sampling and design of RNA-seq of rare minnow oocytes at different developmental stages. B: Heat map showing RNA-seq results for rare minnow oocytes at different stages. r1: repeat 1; r2: repeat 2; r3: repeat 3. Note: One sample from the mid group was removed due to poor quality. C: Volcano plot showing DEGs in rare minnow oocytes between mid and late stages. D: KEGG results showing enriched terms based on DEGs from C.

Generation of transgenic zebrafish lines expressing rare minnow *zp* genes

FLAG-tagged rare minnow *zp* gene infusion with *egfp* under the control of a *zp3.2* promoter was cloned into pT2A plasmids, and co-injected with transposase mRNAs into 1-cell stage of WT zebrafish embryos. Day 16 F0 juveniles were initially screened for GFP signals in the gonads and confirmed by PCR analysis (Figure 2B). F0 founders were raised to adulthood, and GFP-positive ovaries were isolated and examined under a fluorescence microscope. GFP signals were detected in different oocyte and/or oogonial cell stages, depending on the transgenic lines. For instance, GFP was detected in both oogonia and oocytes in Tg(*zp3.2*: *zp3a*-eGFP) and Tg(*zp3.2*: *zp4l*-eGFP) ovaries (Figure 2C; Supplementary Figure S2A). Of note, strong GFP signals were detected in the EE of ovulated eggs from F0 Tg(*zp3.2*: *zp3a*-eGFP) parents (Figure 2D), indicating that the Zp3a-eGFP fusion protein was transferred from the oocyte cytoplasm to EE during oocyte maturation.

F1 embryos were obtained by crossing F0 and WT adults. At day 16, F1 juveniles were screened under a fluorescence microscope, and GFP signals were detected in all four transgenic lines: Tg(*zp3.2*: *zp3a*-eGFP), Tg(*zp3.2*: *zp3*-eGFP), Tg(*zp3.2*: *zp2l2*-eGFP), and Tg(*zp3.2*: *zp4l*-eGFP) (Figure 2E; Supplementary Figure S2B). The GFP signals were predominantly found in the ovaries, in line with previous reports (Liu et al., 2006; Wang & Gong, 1999). As strong GFP signals were found in the EE of ovulated eggs from Tg(*zp3.2*: *zp3a*-eGFP), we performed most subsequent experiments using this line.

To investigate whether the transgenic line stably expressed FLAG-Zp3a-eGFP, EEs were isolated from fertilized F2/F3 eggs and subjected to IF staining using FLAG antibodies. Punctated IF signals were readily detected on the EE of transgenic eggs but not of control eggs (Figure 2F).

Gain of adhesiveness in Tg(*zp3.2*: *zp3a*-eGFP) eggs

We investigated whether adhesiveness was altered in the transgenic eggs. To this end, fertilized eggs from WT and transgenic zebrafish were immediately transferred to Petri dishes or tanks and placed on an orbital shaker. The control eggs floated back and forth, driven by the shaker, whereas most Tg(*zp3.2*: *zp3a-eGFP*) eggs stuck to the bottom of the dish and did not move (Supplementary Movie 1).

Based on the above observations, we next asked whether transgenic eggs gained certain adhesive structures/materials in the outer layer of the EE, similar to that found in rare minnow eggs. First, we examined the adhesive structure of rare minnow EE by TEM. Thread like adhesive substances were detected on the surface of EEs, which primarily consisted of two components: i.e., inner darker electron-dense material and outer lighter (gray) material (Figure 3A; Supplementary Figure S3A, B).

Next, EEs were isolated from control and transgenic eggs at 0, 0.5, and 1 hour post fertilization (hpf) and subjected to TEM

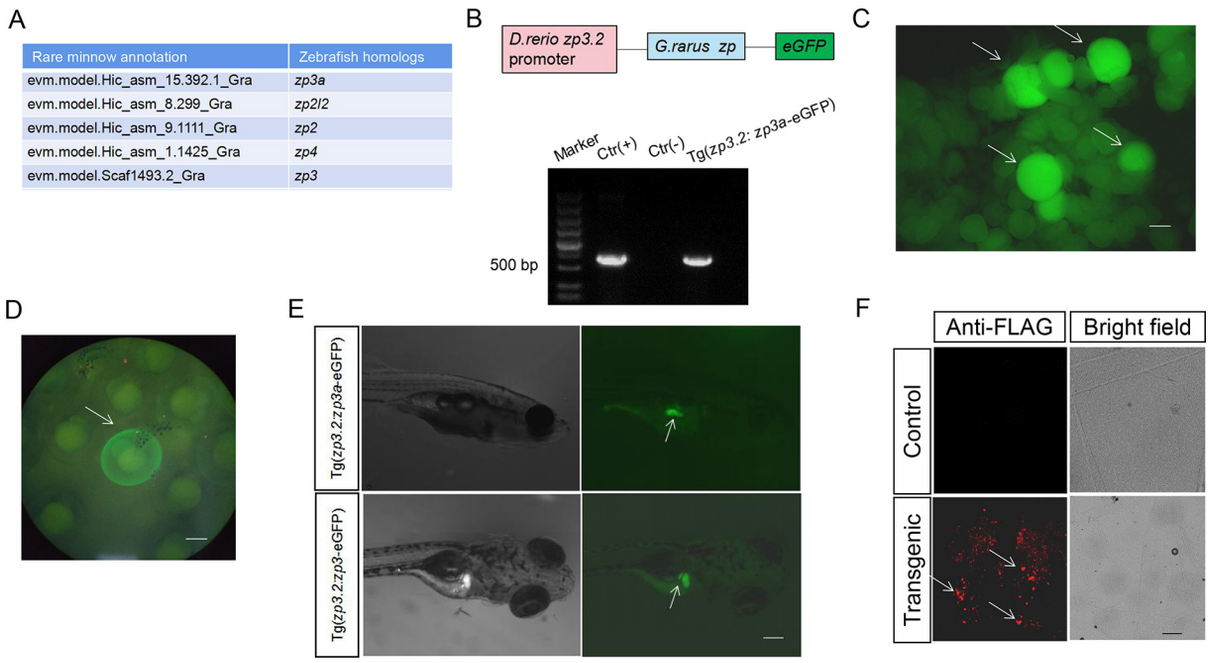

Figure 2 Establishment of transgenic zebrafish lines expressing rare minnow Zps

A: Zp proteins identified in EE of rare minnow by LC-MS/MS. B: Upper: Cartoon showing zebrafish *zp3.2* promoter-rare minnow *zp*-eGFP expression construct; Lower: Gel image showing GFP PCR products amplified from transgenic embryos. Ctr: *zp3.2*: eGFP constructs. C: Fluorescence image showing GFP signals in F0 transgenic ovaries. White arrows indicate oocytes with strong GFP signals. D: Image showing GFP expression in transgenic eggs from F0 parents. White arrow indicates ovulated egg with GFP signals on EE. E: Representative images showing GFP signals in the gonads of indicated transgenic lines. White arrows indicate GFP-positive gonads. F: IF images showing expression of FLAG-tagged Zp3a-eGFP protein in isolated EE of control and transgenic eggs using FLAG antibodies. Note: punctated signals were observed only on EE of transgenic eggs. Bar: 200 μm.

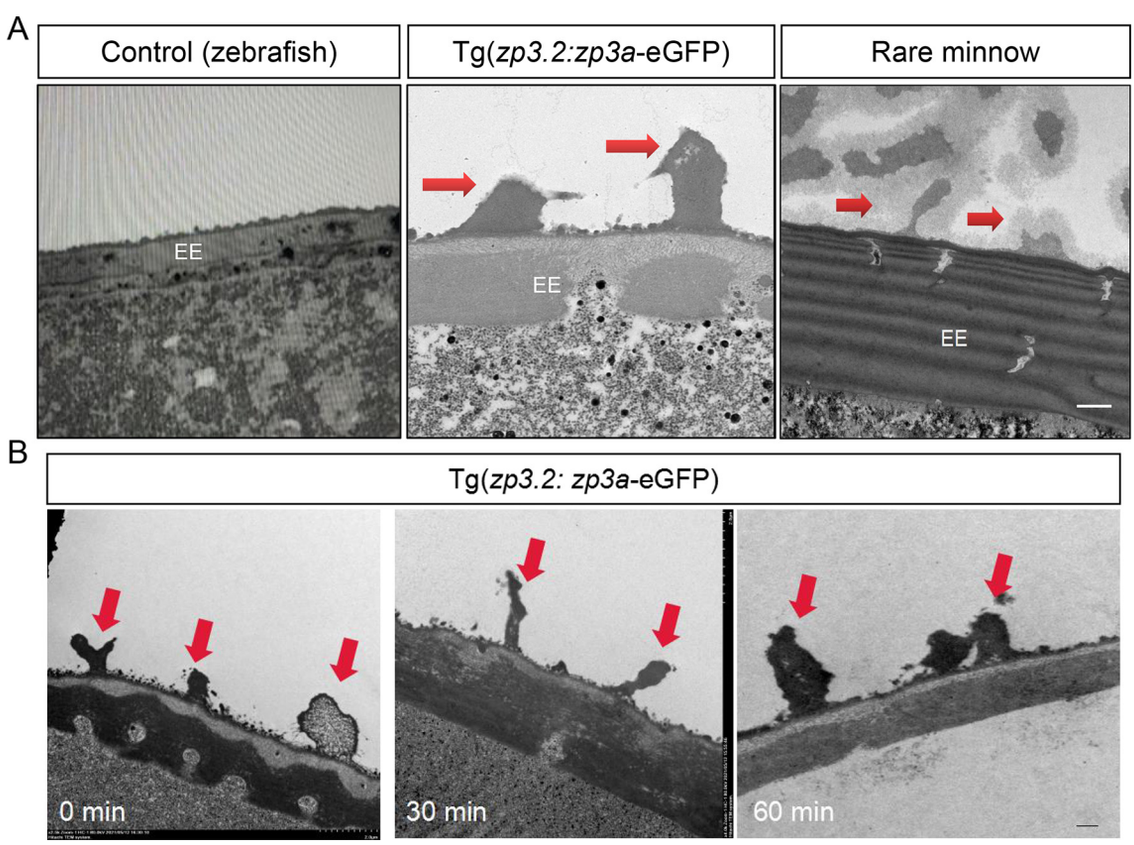

Figure 3 Gain of partial adhesiveness in transgenic zebrafish eggs

A: TEM images showing structures in outer layer of 0 hpf fertilized eggs from WT zebrafish, Tg(*zp3.2: zp3a*-eGFP) line, and rare minnow. Red arrows indicate electron-dense projections. Bar: 2 μm. B: TEM images showing budlike structures on outer layer of transgenic eggs at indicated time points. Red arrows indicate electron-dense projections. Bar: 1 μm.

analysis. In the control group, the EE consisted of three layers and a largely smooth surface. In the transgenic group, the EE also consisted of three layers, but with several bud-like protuberances (electron-dense projections) on the surface (Figure 3A, B), morphologically similar to those in WT rare minnow, although shorter. Based on the morphological and functional data, we tentatively concluded that Tg(*zp3.2*: *zp3a*-eGFP) eggs gained partial adhesiveness, resembling that of rare minnow.

Increased hydration in transgenic zebrafish eggs

Surprisingly, after examining the transgenic eggs, their volume appeared to be larger than that of the controls. Thus, we collected and compared control and transgenic embryos at 0, 0.5, 1, 1.5, 2, 4, and 6 hpf. Under the microscope, egg volume was largely comparable at 0 hpf. However, from 0.5 hpf onwards, average egg volume of the transgenic eggs was significantly larger than that of the controls (Figure 4A; Supplementary Figure S4). We further characterized the eggs by measuring egg and yolk diameter, as well as perivitelline space width. Average egg diameter and perivitelline space width were larger in the transgenic eggs than in the control eggs, whereas average yolk diameter showed the opposite pattern (Figure 4B–D). Interestingly, in the control eggs, significant changes in perivitelline space and egg volume were completed by 0.5 hpf and did not significantly increase thereafter, whereas in transgenic eggs, both increased and peaked at around 2 hpf.

Previous studies have shown that water uptake is the main cause of increased oocyte or egg volume in fish (Cerda et al., 2007). Here, the increased perivitelline space width and egg volume indicated enhanced water uptake or hydration in the transgenic eggs. Therefore, we compared average weight and water loss between transgenic and control eggs at 1 hpf. Results showed that water content was significantly higher in transgenic eggs than in control eggs (Figure 4E, F). Taken together, we concluded that hydration was enhanced in the transgenic eggs.

Gain of buoyancy in transgenic eggs

Based on the above data, we speculated that buoyancy was greater in the transgenic eggs than in the control eggs. To investigate this, we collected control and transgenic eggs at 0, 0.5, 1, 1.5, 2, 4, and 6 hpf, and sank them side by side in a tank filled with egg water. As expected, starting from 0.5 hpf, the transgenic eggs sank more slowly than the control eggs (Figure 5A, B; Supplementary Movie 2). Based on these findings, we concluded that the transgenic eggs acquired partial buoyancy characteristics.

Alteration of yolk cell metabolism in transgenic eggs

In marine species, egg buoyancy is achieved primarily by hydration through degradation of yolk proteins (Fabra et al., 2005). In many freshwater fish, lipid droplets in the yolk cell are thought to contribute to buoyancy (Baras et al., 2018; Chen et al., 2021). Based on the reverse correlation between buoyancy/hydration and yolk cell size, we speculated that abnormal vitellogenin (VTG)/yolk metabolism may occur in the transgenic eggs.

All eggs were first stained with Coomassie brilliant blue at 0 and 1 hpf, showing a reduction in VTG levels in the transgenic eggs compared to the control eggs (Figure 6A). Next, western blot analysis using VTG antibodies for lysates made from 0 and 1 hpf embryos showed that VTG levels were lower in transgenic embryos than in the controls (Figure 6B). These results suggested possible premature and accelerated degradation of VTG.

Next, LC-MS-based non-targeted metabolomics analysis was performed for the control and transgenic eggs at 1 hpf. Principal component analysis (PCA) showed a clear

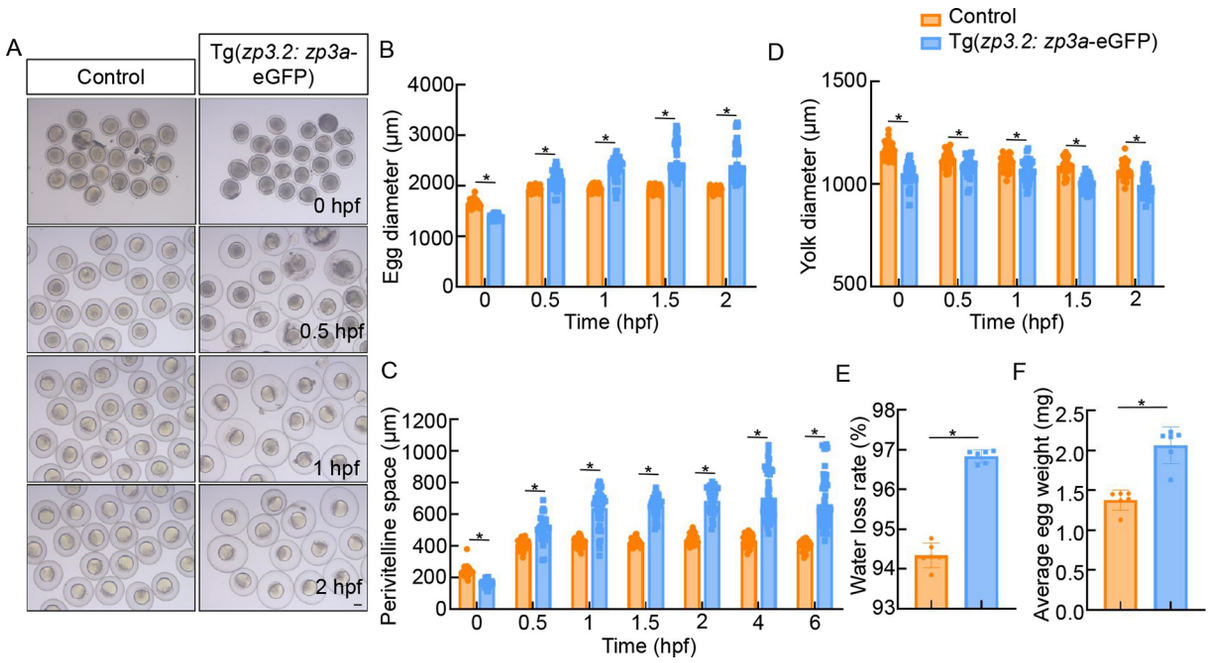

Figure 4 Enhanced hydration in transgenic zebrafish eggs

A: Representative images showing morphology of fertilized control and transgenic eggs at indicated time points. Note: increased volume of transgenic eggs is compared to controls. B–D: Quantitation of egg, yolk, and perivitelline space diameter of control and transgenic eggs at indicated time points. E: Comparison of water loss between control and transgenic eggs at 1 hpf. F: Comparison of average weight of control and transgenic eggs at 1 hpf. Bar: 200 μm. *: $P<0.05$.

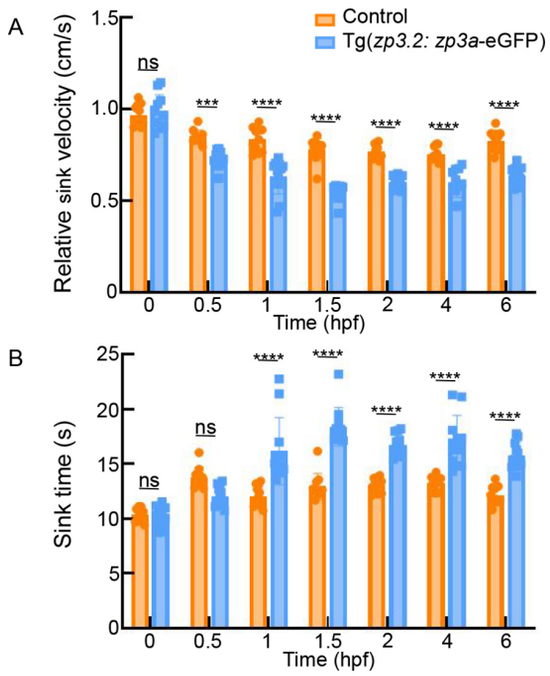

Figure 5 Gain of buoyancy in transgenic zebrafish eggs

A: Bar graph showing relative sink velocity of transgenic and control eggs at the indicated time points. B: Bar graph showing time required to sink from the surface to the bottom of eggs at the indicated time points. Experiments were repeated three times. ns: Not significant; ***: $P<0.001$; ****: $P<0.0001$.

separation between control and transgenic eggs (Figure 6C). Under positive ion mode, approximately 100 compounds were identified as differential metabolites (DMs); under negative ion mode, approximately 90 compounds were identified. The DMs under positive ion mode are shown as a heat map (Figure 6D). KEGG analysis of the DMs revealed enrichment in tricarboxylic acid cycle (TCA) and amino acid, nucleic acid, vitamin, and lipid metabolism. Consistently, variable importance in projection (VIP) analysis showed that the top DMs included all trans-retinoic acids, 5-hydroxy-6E,8Z,11Z,14Z-eico-satetraenoic acid (5-HETE), 5-hydroxy-6E,8Z,11Z,14Z,17Z-eicosapentaenoic acid (5-HEPE), phosphatidylethanolamine, free amino acid (FAAs), glucosamine, galactosamine, adenosine diphosphate (ADP), riboflavin, glutathione, and cis-aconitic acid (Figure 6E; Supplementary Figure S5A–D). Interestingly, spermidine and testosterone were highly represented (Supplementary Figure S5A–C), suggesting that sex hormone levels may be abnormal in transgenic eggs. Taken together, we concluded that VTG/yolk protein metabolism was affected in the transgenic eggs, which may be involved in the change in hydration and buoyancy.

Expression of genes involved in VTG metabolism

VTG metabolism is regulated by a variety of upstream factors, including Na+/K+ ATPase, cysteine proteinase cathepsin L, serine/threonine protein phosphatase, and vacuolar H^+-ATPase (Cerda et al., 2007; Chen et al., 2022). We therefore determined whether the expression of these genes was

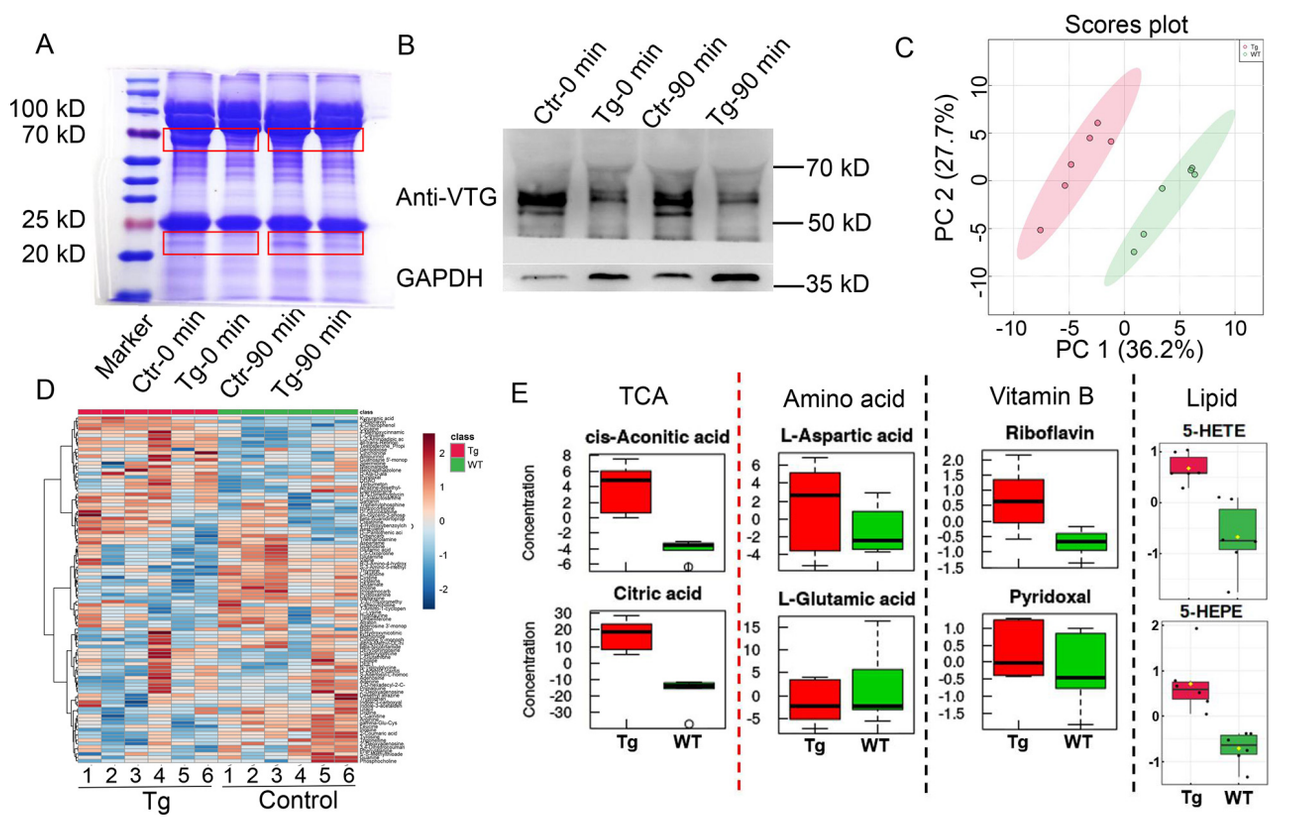

Figure 6 Changes in yolk cell metabolism in transgenic zebrafish eggs

A: Coomassie brilliant blue-stained image showing a reduction in VTG levels in transgenic (TG) eggs compared to controls (Ctr) at indicated time points. Red boxes indicate where bands are obviously altered. B: Western blotting results showing greater reduction in VTG levels in transgenic eggs compared to controls at indicated time points. C: PCA showing clear separation between control and transgenic eggs. D: Heat map showing DMs between control (WT) and transgenic (TG) groups. Six control and transgenic eggs were sampled (numbered 1–6). E: Box plots showing relative concentration of indicated metabolites in indicated groups.

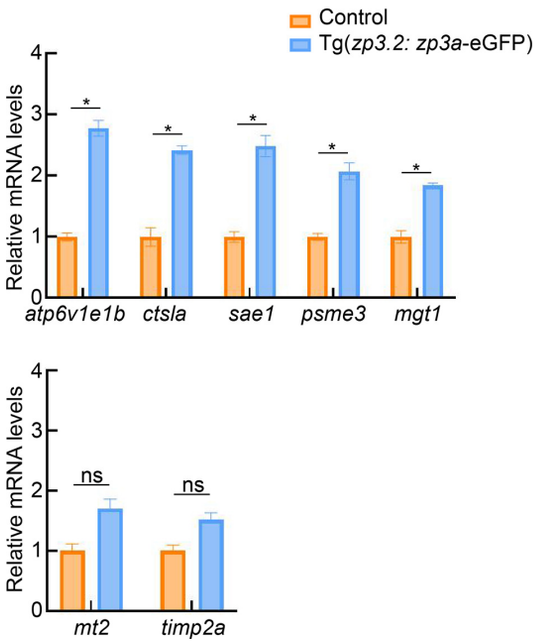

Figure 7 Expression of genes involved in VTG metabolism

A, B: qRT-PCR results showing relative expression of indicated genes in control and transgenic eggs. Experiments were repeated three times. ns: not significant; *: $P<0.05$.

altered in transgenic eggs using quantitative real-time PCR (qRT-PCR) (Figure 7A). Results showed that VTG metabolism-promoting genes, such as *atp6v1e1*, *ctsla*, and *mgt1*, were up-regulated in transgenic eggs, whereas the expression of genes encoding inhibitors of metalloproteinases, such as *mt2* and *timp2a*, were largely comparable between the control and transgenic eggs (Figure 7B). These findings suggested that abnormal metabolism of VTG/yolk proteins may occur in transgenic eggs.

Egg adhesiveness in *zp3a*-deficient rare minnow

We also investigated whether depletion or reduction of Zp3a in rare minnow leads to changes in egg adhesiveness. To this end, we generated *zp3a* mutant rare minnow using CRISPR/Cas9 technology (Figure 8A). We generated two mutant alleles, one bearing a 2 bp deletion and one bearing a 5 bp deletion (Figure 8B). Both mutations were predicted to cause a truncated Zp3a protein of 143 amino acids, resulting in loss of protein function.

Approximately 20 F0 founders bearing mutant alleles were identified and raised to adulthood. After crossing F0 and WT adults, F1 heterozygous mutants were obtained and raised to adulthood. Unfortunately, we had difficulty obtaining homologous mutants. Although offspring were readily obtained by crossing eight-month-old WT rare minnow, few fertilized eggs were obtained when F1 heterozygous adults at the same age were crossed. The ovaries of the F1 heterozygous females were sectioned and H&E stained. No significant differences were found between the heterozygous mutant and control ovaries. Furthermore, oocyte development in the heterozygous mutants appeared normal (Figure 8C).

The ovaries of heterozygous mutant and control rare minnow were subjected to TEM analysis. The development of adhesive substances outside the EE appeared largely normal in the oocytes of the heterozygous mutants compared to the controls (Figure 8D). Thus, these results suggested that adhesiveness was not significantly affected in the ovaries of *zp3a*$^{+/-}$ rare minnow.

DISCUSSION

Upon fertilization, fish eggs absorb water (hydration) to form the perivitelline space, which induces swelling of the EE and leads to egg adhesiveness. This suggests that egg adhesiveness and hydration/buoyancy are inherently linked. However, few studies have investigated this relationship, likely due to the lack of a suitable research model. In the current study, transfer of rare minnow Zp3a resulted in changes in egg adhesiveness and buoyancy in transgenic zebrafish, mimicking the evolutionary history of the spawning habits of endemic East Asian cyprinids, from demersal eggs to semi-buoyant and adhesive eggs. Our findings emphasize the potential role of *zp* genes in the regulation of spawning habits, providing important insights into how endemic East Asian cyprinids may have adapted to the Yangtze river-lake system.

Transgenic zebrafish eggs exhibited gain of partial adhesiveness. This was supported by the emergence of electron-dense projections in the EE surface that were morphologically similar to those found in WT rare minnow and,

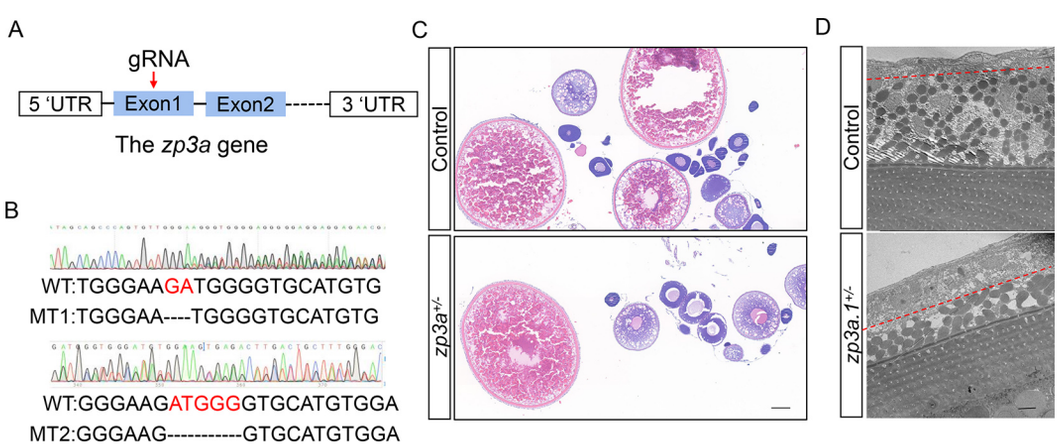

Figure 8 Generation of *zp3a*-deficient rare minnow

A: Cartoon showing targeting site of sgRNA in *zp3a* gene of rare minnow. B: Genotyping results showing −2 bp mutant allele (up) and −5 bp mutant allele (bottom). C: H&E-stained images showing oocyte morphology in control and −5 bp heterozygous ovaries. Bar: 200 μm. D: Representative TEM images showing surface of EEs of control and heterozygous mutant oocytes. Red dashed lines indicate borders between developing adhesive layer and supporting somatic cells. Bar: 10 μm.

more importantly, functional evidence showing that transgenic eggs firmly adhered to each other and to the bottom of the tank. Metabolomics analysis showed that the transgenic eggs contained more glucosamine and galactosamine than control eggs. Glycoprotein and glycosaminoglycan have been shown to contribute to the development of egg stickiness, and glucose, fructose, galactose, and uronic acid are major carbohydrates in the EE of cyprinids (Galliano et al., 2003; Mansour et al., 2009; Riehl and Patzner, 1998; Rizzo et al., 2002).

The transgenic eggs also showed increased buoyancy. As the volume of the perivitelline space increases, the egg becomes larger and its specific gravity decreases. However, the mechanisms underlying the regulation of egg buoyancy in fish remain elusive. In marine environments, most teleost species produce pelagic eggs, which exhibit aquaporin-mediated water uptake during oocyte maturation (Baras et al., 2018). As the osmolality of marine fish oocytes is lower than that of seawater, but higher than that of ovarian fluid, buoyancy is mainly achieved through hydration in the ovaries (Fabra et al., 2005). For freshwater fish, hydration during oocyte maturation is minimal (Cerda et al., 2007), instead occurring after egg ovulation in a hypotonic environment, where egg osmolality is usually higher than that of freshwater. Therefore, the mechanisms underlying egg buoyancy in freshwater fish are somewhat complicated. In addition to hydration, lipid droplets in the yolk are also reported to contribute to buoyancy because they are lighter than water. In the present work, non-targeted metabolomics suggested that both hydration and lipid droplets may contribute to increased buoyancy in the transgenic eggs. First, we observed a significant increase in average egg diameter and perivitelline space width, as well as water content, indicating enhanced hydration. Consistent with this, FAA, carbohydrate, nucleic acid, and vitamin metabolite content was higher in transgenic eggs than control eggs, which may increase egg osmolality. Second, the content and composition of the lipid droplets were altered in the transgenic eggs compared to the controls. Among the important DMs identified, such as 5-HETE, 5-HEPE, and phosphatidylethanolamine, 5-HETE and 5-HEPE are known omega-3 unsaturated fatty acid metabolites. Lipid droplets also exhibit additional functions. In particular, the yolk cell is metabolically active in processing lipids to maintain adenosine triphosphate (ATP) homeostasis during early zebrafish embryogenesis (Fraher et al., 2016). Thus, we speculate that lipid droplets in transgenic eggs may be actively processed for both energy consumption and egg buoyancy (Dutta & Sinha, 2017; Hachicho et al., 2015). Consistent with this, transgenic eggs had higher levels of riboflavin and TCA cycle intermediates than control eggs. Riboflavin forms part of the coenzymes flavin adenine dinucleotide (FAD) and flavin mononucleotide, which participate in oxidation-reduction (redox) reactions in metabolic pathways and in ATP production via the mitochondrial respiratory chain (Averianova et al., 2020). Cis-aconitic acid and citric acid are intermediates of the TCA cycle, which produces ATP and precursors for molecular building blocks (e.g., carbohydrates, lipids, amino acids, and nucleotides) (Tao et al., 2019).

How does exogenous Zp3a transfer affect the adhesiveness and hydration of zebrafish eggs? In most cyprinids, eggs are non-sticky until they come into contact with water, after which they can adhere to each other and to aquatic substrates. Adhesiveness of carp eggs was thought to be induced by factors that diffuse from the perivitelline space through the EE (Chang et al., 2002). However, adhesiveness can be developed not only on intact eggs but also on isolated EEs (Mansour et al., 2009), implying that initiation of egg adhesiveness can be induced by components of the EE itself. As egg stickiness is mediated by glycoproteins such as Zps (Jovine et al., 2002; Sano et al., 2017), expression of rare minnow Zp3a in transgenic zebrafish eggs may trigger certain biological reactions to induce partial viscosity. For instance, N-glycosylation modification in rare minnow Zp3a may contribute to the gain of partial stickiness in transgenic eggs, although this awaits further validation (Boja et al., 2003; Mansour et al., 2009). Another possibility is that introduction of the rare minnow *zp3a* gene simply causes EE malformations in zebrafish, resulting in abnormal yolk accumulation and expansion of perivitelline space. In control eggs, significant changes in the perivitelline space and egg volume were completed by 0.5 hpf, whereas in transgenic eggs, these changes increased and peaked at 2–4 hpf. Furthermore, recent studies have shown that Zp3 can interact with a panel of cytoplasmic proteins, such as Ptprk and Diaph2 (Gao et al., 2017). Ptprk is a receptor-type protein tyrosine phosphatase that regulates key signaling pathways such as Wnt/beta-catenin, and epidermal growth factor receptor (EGFR). Diaph2 has been shown to play a role in the development and maturation of the ovary (Gao et al., 2017). Therefore, expression of rare minnow Zp3a may affect the activities of enzymes involved in the degradation of yolk proteins/VTG or development of oocytes, resulting in enhanced hydration of transgenic eggs.

DATA AVAILABILITY

Raw data were submitted to the NCBI Sequence Read Archive (SRA) database (BioProjectID PRJNA910672), GSA database (PRJCA013771), and Science Data Bank database (DOI:10.57760/sciencedb.j00139.00044, DOI:10.57760/sciencedb.06900).

SUPPLEMENTARY DATA

Supplementary data to this article can be found online.

COMPETING INTERESTS

The authors declare that they have no competing interests.

AUTHORS' CONTRIBUTIONS

Y.Q.C., Y.X.W., and X.H. from Sun Lab performed most experiments. Y.Z. and J.Z. performed the TEM experiments. P.X., J.C., and Y.H.S. supervised the work. Y.H.S. provided the facilities for the work and wrote the manuscript. All authors read and approved the final version of the manuscript.

REFERENCES

Averianova LA, Balabanova LA, Son OM, et al. 2020. Production of vitamin B2 (riboflavin) by microorganisms: an overview. *Frontiers in Bioengineering and Biotechnology*, **8**: 570828.

Baras E, Arifin OZ, Slembrouck J, et al. 2018. Oil globule size in fish eggs: a matter of biome and reproductive strategy. *Fish and Fisheries*, **19**(6): 996−1002.

Boja ES, Hoodbhoy T, Fales HM, et al. 2003. Structural characterization of native mouse zona pellucida proteins using mass spectrometry. *Journal of Biological Chemistry*, **278**(36): 34189−34202.

Bonsignorio D, Perego L, Del Giacco L, et al. 1996. Structure and macromolecular composition of the zebrafish egg chorion. *Zygote*, **4**(2): 101−108.

Cao LX, Huang Q, Wu ZC, et al. 2016. Neofunctionalization of zona pellucida proteins enhances freeze-prevention in the eggs of antarctic notothenioids. *Nature Communications*, **7**: 12987.

Cerda J, Fabra M, Raldua D. 2007. Physiological and molecular basis of fish oocyte hydration. *In*: Babin PJ, et al. (eds.). The Fish Oocyte: From Basic Studies to Biotechnological Applications. Amsterdam, Netherlands: Springer Press, 349–396.

Chang YS, Wang YW, Huang FL. 2002. Cross-linking of ZP2 and ZP3 by Transglutaminase is required for the formation of the outer layer of fertilization envelope of carp egg. *Molecular Reproduction and Development*, **63**(2): 237−244.

Chen F, Smith C, Wang YK, et al. 2021. The evolution of alternative buoyancy mechanisms in freshwater fish eggs. *Frontiers in Ecology and Evolution*, **9**: 736718.

Chen F, Wang YK, He J, et al. 2022. Molecular mechanisms of spawning habits for the adaptive radiation of endemic East Asian cyprinid fishes. *Research*, **2022**: 9827986.

Dutta A, Sinha DK. 2017. Zebrafish lipid droplets regulate embryonic ATP homeostasis to power early development. *Open Biology*, **7**(7): 170063.

Esmaeili HR, Johal MS. 2005. Ultrastructural features of the egg envelope of silver carp, *Hypophthalmichthys molitrix* (osteichthyes, cyprinidae). *Environmental Biology of Fishes*, **72**(4): 373−377.

Fabra M, Raldúa D, Power DM, Deen PMT, Cerdà J. 2005. Marine fish egg hydration is aquaporin-mediated. *Science*, **307**(5709): 545.

Feng CG, Wang K, Xu WJ, et al. 2022. Monsoon boosted radiation of the endemic East Asian carps. *Science China Life Sciences*,doi: 10.1007/s11427-022-2141-1.

Fraher D, Sanigorski A, Mellett NA, et al. 2016. Zebrafish embryonic lipidomic analysis reveals that the yolk cell is metabolically active in processing lipid. *Cell Reports*, **14**(6): 1317−1329.

Galliano M, Minchiotti L, Campagnoli M, et al. 2003. Structural and biochemical characterization of a new type of lectin isolated from carp eggs. *Biochemical Journal*, **376**(2): 433−440.

Gao LL, Zhou CX, Zhang XL, et al. 2017. ZP3 is required for germinal vesicle breakdown in mouse oocyte meiosis. *Scientific Reports*, **7**: 41272.

Hachicho N, Reithel S, Miltner A, et al. 2015. Body mass parameters, lipid profiles and protein contents of zebrafish embryos and effects of 2, 4-dinitrophenol exposure. *PLoS One*, **10**(8): e0134755.

Hu XD, Li HR, Lin YS, et al. 2022. Genomic deciphering of sex determination and unique immune system of a potential model species rare minnow (*Gobiocypris rarus*). *Science Advances*, **8**(5): eabl7253.

Jovine L, Qi HY, Williams Z, et al. 2002. The ZP domain is a conserved module for polymerization of extracellular proteins. *Nature Cell Biology*, **4**(6): 457−461.

Kawakami K, Takeda H, Kawakami N, et al. 2004. A transposon-mediated gene trap approach identifies developmentally regulated genes in zebrafish. *Developmental Cell*, **7**(1): 133−144.

Kong XH, Wang XZ, Gan XN, et al. 2007. The *c-myc* coding DNA sequences of cyprinids (Teleostei: Cypriniformes): implications for phylogeny. *Chinese Science Bulletin*, **52**(11): 1491−1500.

Liu XJ, Wang H, Gong ZY. 2006. Tandem-repeated zebrafish *Zp3* genes possess oocyte-specific promoters and are insensitive to estrogen induction. *Biology of Reproduction*, **74**(6): 1016−1025.

Mansour N, Lahnsteiner F, Patzner RA. 2009. Physiological and biochemical investigations on egg stickiness in common carp. *Animal Reproduction Science*, **114**(1–3): 256–268.

Marques DA, Meier JI, Seehausen O. 2019. A combinatorial view on speciation and adaptive radiation. *Trends in Ecology & Evolution*, **34**(6): 531−544.

McGee MD, Borstein SR, Meier JI, et al. 2020. The ecological and genomic basis of explosive adaptive radiation. *Nature*, **586**(7827): 75−79.

Murray DS, Bain MM, Adams CE. 2013. Adhesion mechanisms in European whitefish *Coregonus lavaretus* eggs: is this a survival mechanism for high-energy spawning grounds?. *Journal of Fish Biology*, **83**(5): 1221−1233.

Niksirat H, Andersson L, Golpour A, et al. 2017. Quantification of egg proteome changes during fertilization in sterlet *Acipenser ruthenus*. *Biochemical and Biophysical Research Communications*, **490**(2): 189–193.

Niksirat H, Levander F, Kouba A, et al. 2020. Proteomic changes after fertilization and before first cleavage in rainbow trout *Oncorhynchus mykiss*. *Aquaculture*, **520**: 734951.

Riehl R, Patzner RA. 1998. Minireview: the modes of egg attachment in teleost fishes. *Italian Journal of Zoology*, **65**(sup1): 415−420.

Rizzo E, Sato Y, Barreto BP, et al. 2002. Adhesiveness and surface patterns of eggs in neotropical freshwater teleosts. *Journal of Fish Biology*, **61**(3): 615−632.

Sano K, Kawaguchi M, Katano K, et al. 2017. Comparison of egg envelope thickness in teleosts and its relationship to the sites of ZP protein synthesis. *Journal of Experimental Zoology Part B:Molecular and Developmental Evolution*, **328**(3): 240−258.

Sun XJ, Wang PX. 2005. How old is the Asian monsoon system? — —Palaeobotanical records from China. *Palaeogeography, Palaeoclimatology, Palaeoecology*, **222**(3–4): 181–222.

Tao TQ, He T, Wang XR, et al. 2019. Metabolic profiling analysis of patients with coronary heart disease undergoing Xuefu Zhuyu decoction treatment. *Frontiers in Pharmacology*, **10**: 985.

Tao WJ, Zou M, Wang XZ, et al. 2010. Phylogenomic analysis resolves the formerly intractable adaptive diversification of the Endemic clade of East Asian cyprinidae (Cypriniformes). *PLoS One*, **5**(10): e13508.

Wang H, Gong ZY. 1999. Characterization of two zebrafish cDNA clones encoding egg envelope proteins ZP2 and ZP3. *Biochimica et Biophysica Acta*, **1446**: 156−160.

Wang N, Wu FX. 2015. New Oligocene cyprinid in the central Tibetan Plateau documents the pre-uplift tropical lowlands. *Ichthyological Research*, **62**(3): 274−285.

Wang YK, Chen F, He J, et al. 2022. Comparative ultrastructure and proteomics of two economic species (common carp and grass carp) egg envelope. *Aquaculture*, **546**: 737276.

Zheng HB. 2015. Birth of the Yangtze River: age and tectonic-geomorphic implications. *National Science Review*, **2**(4): 438−453.